

## Accepted Manuscript

A red-emitting fluorescent probe with large Stokes shift for real-time tracking of cysteine over glutathione and homocysteine in living cells

Ming Qian, Liuwei Zhang, Jingyun Wang, Xiaojun Peng



PII: S1386-1425(19)30169-6  
DOI: <https://doi.org/10.1016/j.saa.2019.02.050>  
Reference: SAA 16826

To appear in: *Spectrochimica Acta Part A: Molecular and Biomolecular Spectroscopy*

Received date: 16 September 2018  
Revised date: 16 January 2019  
Accepted date: 16 February 2019

Please cite this article as: M. Qian, L. Zhang, J. Wang, et al., A red-emitting fluorescent probe with large Stokes shift for real-time tracking of cysteine over glutathione and homocysteine in living cells, *Spectrochimica Acta Part A: Molecular and Biomolecular Spectroscopy*, <https://doi.org/10.1016/j.saa.2019.02.050>

This is a PDF file of an unedited manuscript that has been accepted for publication. As a service to our customers we are providing this early version of the manuscript. The manuscript will undergo copyediting, typesetting, and review of the resulting proof before it is published in its final form. Please note that during the production process errors may be discovered which could affect the content, and all legal disclaimers that apply to the journal pertain.

**A red-emitting fluorescent probe with large Stokes shift for real-time tracking of cysteine over glutathione and homocysteine in living cells**

Ming Qian<sup>a,b</sup>, Liuwei Zhang<sup>b</sup>, Jingyun Wang<sup>a,b,\*</sup>, Xiaojun Peng<sup>a</sup>

<sup>a</sup> *State Key Laboratory of Fine Chemicals, Dalian University of Technology, 116024, Dalian, Liaoning, P. R. China*

<sup>b</sup> *School of Life Science and Biotechnology, Dalian University of Technology, 116024, Dalian, Liaoning, P.R. China*

**Abstract:**

Fluorescent probes with high quality for highly selective detection of cysteine (Cys) are still urgently in demand because of the indispensable roles Cys plays in the biological systems. Herein, a red-emitting fluorescent probe **CP** was developed for the highly selective detection of Cys over glutathione (GSH) and homocysteine (Hcy) by incorporating acryloyl group as the recognition unit into the 2-(2-(4-hydroxystyryl)-6-methyl-4H-pyran-4-ylidene) malononitrile (**P-OH**) fluorophore which is characterized by red emission, noteworthy Stokes shift, and appreciable photostability. Basically, **CP** demonstrated appreciable sensing performance toward Cys including short response time of 4 min, high sensitivity with approximately 147-fold emission enhancement, low detection limit of 41.696 nM, and good selectivity both in the solution and living cells, indicating its promising potential of visualizing Cys in biological systems.

Keywords: Fluorescent probe, Cysteine detection, Large Stokes shift, Fluorescence imaging.

**Introduction:**

Cysteine (Cys), regarded as one of the significant biothiols in living systems, play a crucial role in multiple physiological processes including the protein

biosynthesis, mitochondrial protein turnover, metabolism regulation and detoxification administration<sup>1-3</sup>. It was reported that the normal intracellular level of Cys is in the range of 30-200  $\mu\text{M}$ <sup>4</sup> and an abnormal level of Cys is associated with many syndromes such as Alzheimer's disease, liver damage, metabolic hair depigmentation and weakness<sup>5-7</sup>. In view of the crucial physiological and pathological roles Cys plays in biological systems, it is essential to develop an invasive analytical tool for selective Cys detection so as to better elucidate the physiological processes of Cys and understand the specific pathogenesis of Cys-related diseases. So far, fluorescence analysis technique has been widely used in the investigation of intermolecular interactions (such as between drug with human serum albumin, hemoglobin or DNA)<sup>8-13</sup>, and detection of different analytes<sup>14-17</sup>. Fluorescence detection based on small-molecular fluorescent probes that are capable of interacting with the specific analyte to trigger fluorescent signal variation has attracted extensive attention due to their inherent advantages including simplicity for implementation, high sensitivity, good selectivity, and invasive in-situ detection in living systems<sup>18-20</sup>. Among the reported fluorescent probes for the detection of various analytes, specific reaction-based fluorescent probes that possess faster response, higher sensitivity toward targeted analytes have attracted a great deal of attention. Over the past decade, a large number of reaction-based fluorescent probes have been developed for biothiols detection on the basis of several sensing strategies including Michael addition<sup>21-24</sup>, cyclization reaction with the aldehyde<sup>25-27</sup>, cleavage of disulfide<sup>28</sup> and sulfonyl ester<sup>29-31</sup>. Unfortunately, up to now, few reported fluorescent probes could distinguish Cys from homocysteine (Hcy) and glutathione (GSH). Considering the fact that the biothiols possess structural similarity, comparable reactivity, different amounts in biological systems, distinct physiological and pathological functions, it is of great challenges and significance to design brilliant fluorescent probe for discriminating Cys from other two biothiols in living systems<sup>32</sup>. Despite some advancement has been obtained in terms of fluorescent probe design for selective detection of Cys, there

remain some limitations waiting to be overcome to get the further application. Firstly, some reported probes usually show relatively slow response rate or low signal-to-noise ratio in the detection process, which is not favorable for real-time tracking of Cys in living systems<sup>33,34</sup>. Besides, several fluorescent probes exploiting fluorophores that emit fluorescence with a relatively short wavelength (< 600 nm) generally suffer from the auto-fluorescence interference of intrinsic biologically-related species<sup>35-42</sup>. Furthermore, certain reported long-wavelength fluorescent probes that possess short Stokes shift (< 100nm) characterized by the substantial overlap of excitation and emission bands are subjected to self-absorption effect and unsatisfactory anti-interference capability<sup>43-45</sup>. Accordingly, developing long-wavelength fluorescent probe with noteworthy Stokes shift for selective Cys detection with rapid response and high sensitivity is still desirable for the practical application.

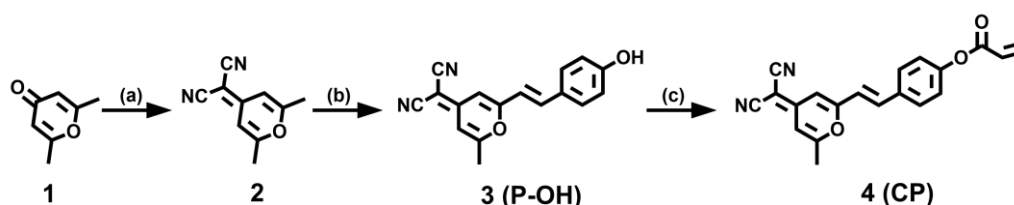
Herein, in this study, a novel red-emitting fluorescent probe (named as **CP**) with large Stokes shift was designed and synthesized for highly selective Cys detection in living cells by introducing acryloyl group as the recognition group into the 2-(2-(4-hydroxystyryl)-6-methyl-4H-pyran-4-ylidene) malononitrile fluorophore (**P-OH**)<sup>46-48</sup>. Basically, the probe itself exhibits almost no fluorescence emission due to the fluorescence masking effect of the acryloyl group. Upon recognizing with Cys, **CP** will undergo the Michael addition between Cys and the acryloyl group to afford a transient intermediate, followed by the intramolecular cyclization to release **P-OH** fluorophore with strong red fluorescence. Accordingly, Cys was detected by monitoring the changes of fluorescence intensity before and after the reaction. As expected, this probe demonstrated excellent sensing properties toward Cys as expected. Firstly, probe **CP** demonstrated good selectivity for Cys over various analytes, especially, Hcy and GSH. Secondly, the probe exhibited short response time of 4 min toward Cys in the solution. Thirdly, this probe had high signal-to-noise ratio of 147-fold and high sensitivity with the ultralow detection limit of 41.696 nM. Lastly,

**CP** was successfully applied to monitor the Cys level in living cells with low cytotoxicity. To sum up, probe **CP** emerged as a promising reaction-based fluorescent probe for the highly selective detection of Cys in living cells.

## 2. Materials and methods

### 2.1. Instruments and materials

All reagents used were obtained from commercial suppliers and used directly without further purification unless otherwise stated. The synthesized compounds were characterized by three different analysis method including high-resolution mass spectra (HRMS),  $^1\text{H}$  NMR and  $^{13}\text{C}$  NMR. HRMS were obtained by the LTQ Orbitrap XL mass spectrometer.  $^1\text{H}$  NMR and  $^{13}\text{C}$  NMR spectra were recorded in Deuterium reagents by a Bruker Avance II 500 spectrometer with tetramethylsilane (TMS) as an internal standard. All reactions were monitored using thin-layer chromatography (TLC) which was performed on silica gel plates (60F-254). Column chromatography was carried out on silica gel (200~300 mesh) obtained from Qingdao Ocean Chemicals. The deionized water used for experiments was purified by a Millipore-Q system (Millipore, USA). UV-vis absorption spectra and fluorescence emission spectra were obtained employing an Agilent Cary 60 UV-vis spectrometer and Agilent Cary Eclipse fluorescence spectrophotometer respectively using a 10 mm standard quartz cuvette. Fluorescence images were obtained by confocal laser scanning microscopy (Fluoview1200, Olympus, Japan) with a  $100\times$  objective lens.



**Scheme 1.** The synthetic route of probe **CP**. Reaction conditions: (a) malononitrile,

acetic anhydride, reflux; (b) p-hydroxybenzaldehyde, piperidine, acetonitrile, reflux; (c) acryloyl chloride, DIEPA, 0 °C, anhydrous dichloromethane;

## 2.2. Synthesis and Characterization

### 2.2.1 The synthesis of 2-(2-(4-hydroxystyryl)-6-methyl-4H-pyran-4-ylidene) malononitrile fluorophore (**P-OH**)

Compound **2** (516 mg, 3 mmol)<sup>49</sup> and 4-hydroxybenzaldehyde (185 mg, 1.5 mmol), piperidine (0.3 ml) was added in 10 ml acetonitrile. The mixture was refluxed for 6 h under N<sub>2</sub> atmosphere. After the removal of the solvent, the residue was dissolved with dichloromethane, washed with brine and deionized water three times respectively, then the obtained organic phase was dried over Na<sub>2</sub>SO<sub>4</sub>. Subsequently, the solvent was evaporated under reduced pressure to get the crude product, and the crude product was purified by silica column chromatography (dichloromethane: ethyl acetate = 100:5, v/v) to give an orange solid (42.7%). <sup>1</sup>H NMR (500 MHz, DMSO-d<sub>6</sub>) δ 10.05 (s, 1H), 7.55 (d, J = 8.6 Hz, 2H), 7.46 (d, J = 16.1 Hz, 1H), 7.12 (d, J = 16.1 Hz, 1H), 6.86 – 6.79 (m, 3H), 6.66 (d, J = 1.3 Hz, 1H), 2.45 (s, 3H). <sup>13</sup>C NMR (DMSO-d<sub>6</sub>): δ 163.89, 160.46, 159.72, 156.69, 137.84, 129.96, 125.94, 115.93, 115.54, 115.39, 105.88, 105.66, 55.00, 19.35. HRMS: calculated for [M-H]<sup>-</sup>: 275.0821; found: 275.0827.

### 2.2.2 The synthesis of the probe **CP**

**P-OH** (82.8 mg, 0.3 mmol), triethylamine (0.42 ml, 3 mmol) were dissolved in 10 ml anhydrous dichloromethane and stirred at 0 °C for 10 min, then acryloyl chloride (54 mg, 0.6 mmol) was added dropwise. After reaction for 30 min, the mixture was allowed to stir at room temperature for another 30 min. Afterwards, the obtained solution was diluted with 50 ml dichloromethane and washed with brine and distilled water for three times respectively, then dried over anhydrous Na<sub>2</sub>SO<sub>4</sub>. After

the removal of the solvent, the crude product was purified by silica gel chromatography using dichloromethane as the eluent to get the pure target product **CP** as a yellow solid (62%).  $^1\text{H}$  NMR (500 MHz, DMSO- $d_6$ )  $\delta$  7.78 (d,  $J$  = 8.7 Hz, 1H), 7.57 (d,  $J$  = 16.2 Hz, 1H), 7.43 – 7.32 (m, 1H), 7.29 (d,  $J$  = 8.6 Hz, 1H), 6.92 (d,  $J$  = 2.2 Hz, 1H), 6.72 (d,  $J$  = 1.4 Hz, 0H), 6.56 (dd,  $J$  = 17.3, 1.3 Hz, 1H), 6.42 (dd,  $J$  = 17.2, 10.3 Hz, 1H), 6.18 (dd,  $J$  = 10.3, 1.3 Hz, 1H), 2.47 (s, 1H).  $^{13}\text{C}$  NMR (DMSO- $d_6$ ):  $\delta$  164.67, 164.43, 160.08, 157.18, 151.92, 136.94, 134.39, 133.21, 129.64, 127.98, 122.92, 119.85, 115.84, 107.74, 106.41, 56.53, 19.89. HRMS: calculated for  $[\text{M-H}]^-$ : 329.0926; found: 329.0940.

### 2.3. General procedure for spectral measurements

The stock solution of probe **CP** (1 mM) was prepared by adding 1.65 mg pure **CP** solid in 5 ml  $\text{CH}_3\text{CN}$  and maintained in the refrigerator at 4 °C for future use. For the selectivity experiments, stock solutions of biologically relevant analytes were prepared in distilled water. The fluorescence spectra of the resultant solution and the **P-OH** fluorophore were measured using the excited wavelength of 500 nm. The excitation slit width and emission slit width were fixed to 10 nm and 5 nm, respectively. For the investigation of pH effects, the pH was accurately adjusted using dilute hydrochloric acid solution and dilute sodium hydroxide solution and measured with a Model PHS-3C meter.

### 2.4. Cell culture and cytotoxicity assay

Cells were purchased from the Cell Bank of Shanghai Institute of Biochemistry and grown in Dulbecco's modified Eagle's medium (DMEM) supplemented with 10% Fetal Bovine Serum (FBS) and 1% antibiotics. The culture was conducted in a cell incubator under humidified environment of 5%  $\text{CO}_2$  and 37 °C. To conduct the cytotoxicity assay<sup>50</sup>, traditional MTT method was applied based on the mechanism that succinate dehydrogenase in mitochondria of living cells can reduce exogenous MTT to water-insoluble blue-purple crystalline methylene (Formazan) and deposit in

cells, and the amount of formed formazan crystal was associated with the cell viability. Briefly, HeLa cell lines were seeded into a 96-well plate with culture media (100  $\mu$ l) for overnight culture, then cells were incubated with different concentrations of **CP** (0, 2, 4, 6, 8, 10  $\mu$ M) for 24 h. Next, 10  $\mu$ l MTT solution (5 mg/ml) was added to each well. After incubation for 4 h, the culture media was discarded and 100  $\mu$ l of dimethyl sulfoxide (DMSO) was added to dissolve produced formazan. Untreated cells in culture medium were used as the blank control. Finally, the OD value at 570 nm and 630 nm were measured with a microplate reader.

### 2.5. Cellular imaging

For confocal luminescence imaging<sup>51</sup>, HeLa cells in culture media (2 ml) were seeded on 35 mm glass-bottomed dishes at a density of  $1 \times 10^5$  cells per dish. After the overnight culture, the cells were incubated with N-ethylmaleimide (NEM), probe **CP**, biothiols and  $H_2O_2$  respectively according to the specific experiments. Fluorescence images were obtained by confocal laser scanning microscopy (Fluoview1200, Olympus, Japan) with the excitation wavelength of 488 nm.

## 3. Results and discussion

### 3.1. Design and synthesis of probe **CP**

The probe **CP** was designed by employing **P-OH** as the fluorophore and acryloyl moiety as the recognition unit. Fluorophore **P-OH** was picked up due to its red emission properties, large Stokes shift of 141 nm (Figure S1) and excellent photostability (Figure S2). On the other hand, the acryloyl group was selected because it is not only an effective fluorescence quencher but also an excellent recognition moiety that could react with Cys selectively through the Michael addition and the intramolecular cyclization to release the fluorophore **P-OH**. As shown in Scheme 1, **CP** can be readily synthesized from the reaction of **P-OH** with the commercially available acryloyl chloride in the presence of triethylamine. Detailed synthetic

procedures are provided in the experimental section. The structure of **P-OH** and **CP** were successfully confirmed by  $^1\text{H}$  NMR,  $^{13}\text{C}$  NMR, and HRMS provided in the supporting information.

### 3.2. Time-dependent optical responses toward Cys

With probe **CP** in hand, its optical sensing performance toward Cys was firstly investigated by measuring the time-dependent spectra changes in PBS-DMSO (pH=7.4, 1:1) solution. As demonstrated in Figure 1a, the probe itself exhibited a maximum absorption peak at 390 nm. However, with the addition of 50  $\mu\text{M}$  Cys, the initial absorption peak of **CP** vanished gradually within 10 min, along with the simultaneous emergence of two new intensified absorption peak at 425 nm and 500 nm which are consistent with the phenol form absorption peak and phenolate form absorption peak of fluorophore **P-OH**, respectively (Figure S6a). In addition, as shown in Figure S3, the color of the reaction mixture changed from pale yellow to brown, demonstrating that this detection behavior of the probe for Cys could be observed by the naked-eye. As for the time-dependent fluorescence spectra of **CP** toward Cys, it could be observed in Figure 1b that the fluorescence intensity at 641 nm enhanced gradually as the reaction time increased and it reached the saturation within 4 min. This quite short reaction time indicates a fast response behavior of **CP** toward Cys and is much favorable for Cys detection. Additionally, this fluorescence response behavior could also be observed under a 365 nm UV-lamp (Figure S3).

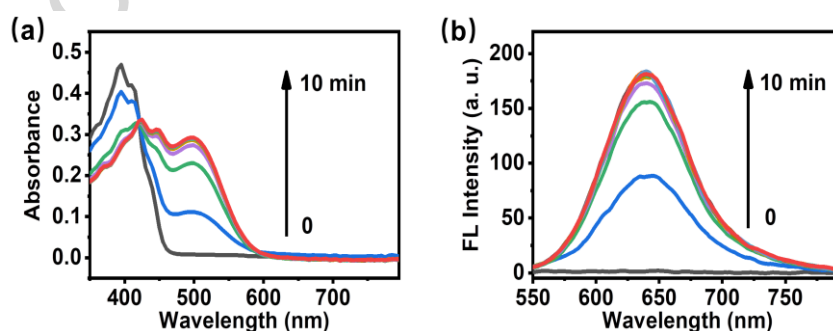


**Figure 1.** The time-dependent response behavior of **CP** toward Cys in PBS-DMSO solution (pH=7.4, 1:1). (a) The time-dependent absorption spectra change in 10 min upon the addition of 50  $\mu\text{M}$  Cys. (b) The time-dependent fluorescence spectra change in 10 min upon the addition of 50  $\mu\text{M}$  Cys.

### 3.3. Fluorescence titration toward Cys

Subsequently, to evaluate the detection sensitivity of **CP** toward Cys, the fluorescence titration experiment was conducted by measuring the fluorescence change of **CP** toward different Cys concentrations in the range of 0-50  $\mu\text{M}$ . It was observed in Figure 2a that **CP** presented a notable fluorescence intensity enhancement at 641 nm gradually toward the increasing amount of Cys and reached the plateau with a 147-fold fluorescence enhancement upon the addition of 20  $\mu\text{M}$  Cys. Furthermore, it is worth noting that the fluorescence intensity at 641 nm was found to be linearly proportional to the Cys concentration in the range of 0-6.0  $\mu\text{M}$  ( $R^2=0.998$ ) with a low detection limit of 41.696 nM which was calculated according to the formula of  $DL=3\sigma/k^{52}$ , demonstrating that probe **CP** has high sensitivity for detecting Cys quantitatively in the *in vitro* measurements (Figure 2b).

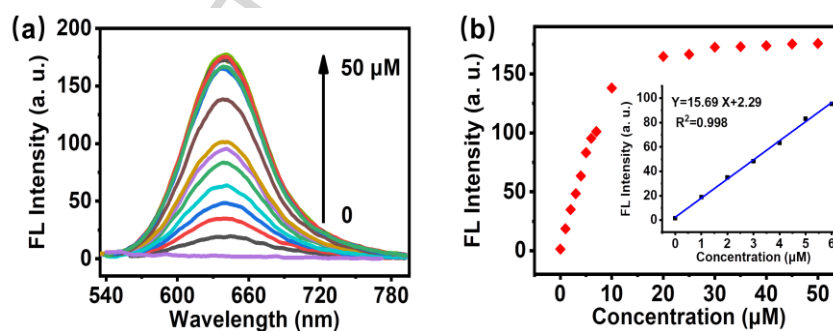


**Figure 2.** The fluorescence titration behavior of **CP** toward Cys in PBS-DMSO solution (pH 7.4, 1:1). (a) The fluorescence spectra change of 10  $\mu\text{M}$  **CP** with addition of different Cys concentrations (0, 1, 2, 3, 4, 5, 6, 7, 10, 15, 20, 25, 30, 40, 45, 50  $\mu\text{M}$ ) for 10 min. (b) The fluorescence intensity at 641 nm changes with the different Cys concentrations (0-50  $\mu\text{M}$ ), inset: the linear relationship between the

fluorescent intensity at 641nm and the low concentration of Cys from 0 to 6  $\mu\text{M}$ .

### 3.4. Discriminating Cys over GSH and Hcy

Taking into consideration that Hcy and GSH are the most likely interferences for Cys detection, the discrimination ability of **CP** for Cys over these two biothiols was firstly investigated. As shown in Figure 3, with the addition of 50  $\mu\text{M}$  Cys, the emission intensity at 641 nm showed a rapid and great fluorescence enhancement at first and reached the maximum within 4 min. By contrast, the addition of 50  $\mu\text{M}$  Hcy or 50  $\mu\text{M}$  GSH induced slight fluorescence intensity change at 641 nm. Moreover, within the same incubation time (4 min), the fluorescence intensity induced by Hcy or GSH is 1:11 and 1:18 in ratio when compared with Cys, indicating the low reactivity kinetic characteristic of **CP** toward GSH and Hcy (Figure S5). Noting that the inherent amount of GSH in living systems is usually in the extremely high level of millimole. Therefore, the response behavior of **CP** toward 1 mM GSH was investigated. As shown in Figure S6, the treatment of 1 mM GSH showed tiny fluorescence alternation with a more time-consuming manner. Based on these results, probe **CP** exhibited higher reactivity and selectivity for Cys over Hcy and GSH.

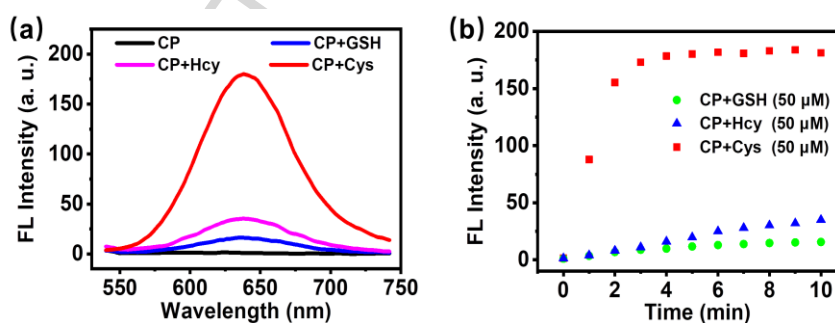


**Figure 3.** The ability of **CP** for discriminating Cys from GSH and Hcy. (a) The fluorescence spectra change of **CP** toward 50  $\mu\text{M}$  GSH, 50  $\mu\text{M}$  Cys, 50  $\mu\text{M}$  Hcy in PBS-DMSO buffer (pH = 7.4, 1: 1). (b) Time-dependent fluorescence intensity change at 641 nm toward 50  $\mu\text{M}$  GSH, 50  $\mu\text{M}$  Cys, 50  $\mu\text{M}$  Hcy in PBS-DMSO buffer (pH = 7.4, 1: 1)

### 3.5. Selectivity over other biological analytes

To further evaluate the selectivity of **CP** toward Cys, the fluorescence response behavior of **CP** toward other physiological amino acids was investigated. As shown in Figure 4, only the addition of Cys (100  $\mu$ M) could induce **CP** to display an obvious response with enhanced fluorescence signal. By contrast, other 19 amino acids (100  $\mu$ M) resulted in negligible fluorescence at 641 nm when compared with Cys. And the specific intensity ratio between other amino acids and Cys (other amino acids : Cys) was determined as follows: 1:49(Asp), 1:36(Gly), 1:53(Glu), 1:59(Ala), 1:34(Trp), 1:33(Ser), 1:33(Val), 1:53(Ile), 1:32(Pro), 1:31(Phe), 1:31(Met), 1:42(Tyr), 1:41(His), 1:46(Thr), 1:58(Leu), 1:40(Asn), 1:37(Gln), 1:32(Lys), 1:31(Arg). Basically, the above fluorescence intensity ratios were all less than 1:30, which indicated the good selectivity of **CP** toward Cys. Furthermore, the competitive experiment suggested that the other amino acids exerted almost no fluorescence intensity alternation, demonstrating that the co-existence of other amino acids didn't interfere with the recognition and detection of Cys by probe **CP**. In a word, **CP** showed excellent selectivity toward Cys over other analytes and is feasible for the selective detection and bioimaging of Cys in living systems.

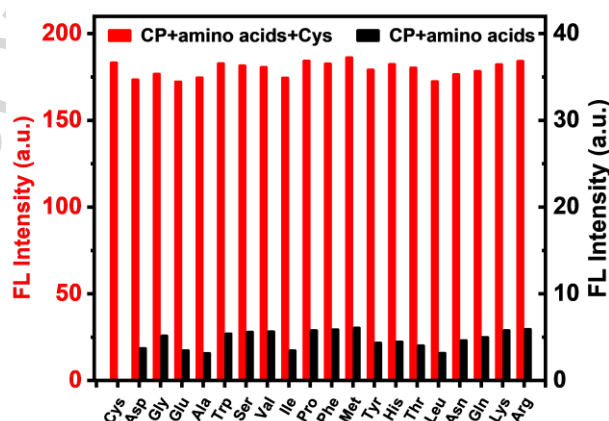


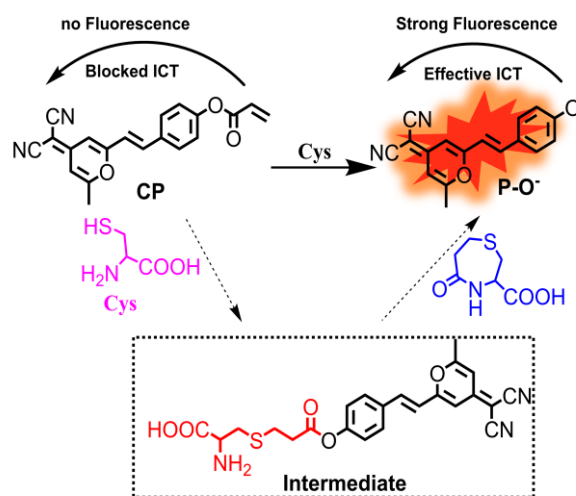
**Figure 4.** The sensing performance of 10  $\mu$ M **CP** toward other 19 amino acids (100

$\mu\text{M}$ ) in PBS-DMSO buffer ( $\text{pH} = 7.4$ , 1:1) in the absence (black bars, the y-axis of black bars is on the right) and presence (red bars, the y-axis of black bars is on the left) of  $50 \mu\text{M}$  Cys.

### 3.6. Verifying the sensing mechanisms

Firstly, as observed in Figure S7, the fluorescence spectra of the reaction solution were consistent with that of the fluorophore **P-OH**, which basically indicated that **P-OH** was indeed released during the sensing process. To further explore the sensing mechanism of **CP** toward Cys, the mass spectroscopy analysis was employed to analyze the product released from the reaction process. As demonstrated in Figure S8, predominantly, three  $[\text{M-H}]^-$  peak at  $m/z$  119.98, 174.01, 275.15 were observed, which were assigned to the Cys ( $M_r = 121.02$ ), the released seven-membered ring cyclic amide by-product ( $M_r = 175.03$ ) and **P-OH** ( $M_r = 276.09$ ) respectively. On the basis of the above results and the reported literatures<sup>53,54</sup>, a proposed<sup>3</sup> sensing mechanism of **CP** toward Cys was outlined in Scheme 2. Specifically, the reaction started with a nucleophilic addition of Cys to the  $\alpha$ ,  $\beta$ -unsaturated carbonyl group of probe **CP** to form the intermediate. Subsequently, this transient intermediate would undergo the free amino-group mediated intramolecular cyclization process to produce the fluorophore **P-OH** accompanied by the release of the seven-membered ring cyclization product simultaneously. Based on the proposed sensing mechanism, the different response behavior of **CP** toward biothiols could be reasonably explained. Basically, the intramolecular cyclization process is no doubt the rate-limiting step during the reaction process. Compared with Hcy, Cys could induce the more kinetically favorable formation of a seven-membered ring product rather than the kinetically disfavored eight-membered ring (the possible product for Hcy) and thus resulted in the faster response behavior. On the other hand, GSH could only generate

the conjugated thioether rather than conducting the intramolecular cyclization reaction due to the hindrance effect of the bulk volume of GSH itself.



**Scheme 2.** Proposed sensing mechanism of **CP** toward Cys.

### 3.7. The effect of pH

Afterwards, the pH effect on **CP** in the absence or presence of Cys was evaluated to validate whether this probe is appropriate for the Cys detection in living systems. As displayed in Figure 5, for the probe **CP**, the fluorescence intensity at 641 nm exhibited almost no change over the pH range of 3.0–9.0, indicating that probe **CP** is pH-unaffected and has good stability in a wide pH range. However, upon the addition of Cys, an obvious enhancement of fluorescence intensity was observed in the pH range of 6.0–9.0, which was attributed to the fact that the high pH environment would boost the deprotonation of **P-OH** fluorophore to produce more deprotonated **PM-O<sup>-</sup>** which is the truly effective form responsible for the red fluorescence emission. In a word, the results above indicated that **CP** can work smoothly over a wide pH range and is suitable for biological applications.

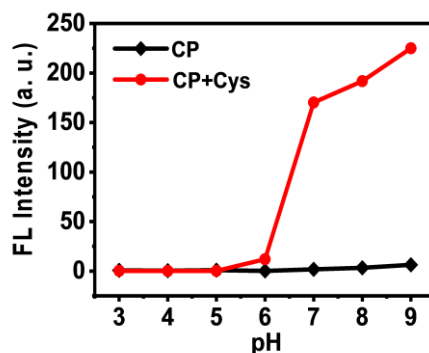


**Figure 5.** The fluorescence intensity of 10  $\mu\text{M}$  **CP** at 641 nm under different pH values (from 3.0 to 9.0) in the absence and presence of 50  $\mu\text{M}$  Cys.

### 3.8. Fluorescence imaging of Cys in living cells

On account of the excellent sensing performance in the solution, the practical application of **CP** in living cells was evaluated by confocal fluorescence microscope. Before the conduction of confocal fluorescence imaging, cytotoxicity test against HeLa cells was carried out to investigate the biocompatibility of the **CP**. As shown in the Figure S9, the viability of HeLa cells maintained to be more than 90% upon the incubation with 0–10  $\mu\text{M}$  of **CP** for 24 h, suggesting that **CP** possess low cytotoxicity against the living cells and was safe enough to be used for the bioimaging of Cys. Subsequently, the practical application of **CP** for Cys detection in confocal fluorescence imaging was carried out in the HeLa cells. As demonstrated in Figure 6, with merely the addition of probe **CP**, red fluorescence was observed in the cytoplasm with the excitation wavelength of 488 nm. Nevertheless, when treated with a recognized biothiols consumption agent (N-ethylmaleimide, NEM)<sup>55</sup> prior to the addition of **CP**, basically no fluorescence signal was observed due to the consumption of intramolecular Cys. The results above indicated that **CP** could be internalized into HeLa cells and response with the basal Cys. Furthermore, upon the exogenous addition of 50  $\mu\text{M}$  Cys, 50  $\mu\text{M}$  Hcy, 1 mM GSH to the NEM-pretreated HeLa cells

respectively, only the treatment of Cys induced distinct red fluorescence signal that is about 7:1 in ratio compared to GSH and 20:1 in ratio for Hcy, furtherly indicating the highly specific response behavior of **CP** toward Cys over GSH and Hcy in living cells. Taking the above results together, we can draw the conclusion that **CP** could detect and visualize both exogenous and endogenous Cys in living cells through a highly specific manner. In addition, the treatment of 100  $\mu\text{M}$   $\text{H}_2\text{O}_2$  resulted in the attenuation of the red fluorescence signal due to the decrease of the intracellular Cys concentration induced by the oxidation of  $\text{H}_2\text{O}_2$ , suggesting that probe **CP** could be exploited as an effective tool for monitoring the level of intracellular Cys. Finally, we attempted to validate whether **CP** could achieve real-time detection of Cys in living cells. As displayed in Figure S10, upon the exogenous addition of 50  $\mu\text{M}$  Cys to the NEM-pretreated HeLa cells, with the increase of incubation time at an interval of 5 minutes, the red fluorescence intensity enhanced increasingly and reached a steady state after 20 min, implying that **CP** is capable of real-time tracking the Cys level in living cells. To sum up, these findings above suggested that probe **CP** could be a feasible tool to monitor the level of Cys via a rea-time and highly selective manner.

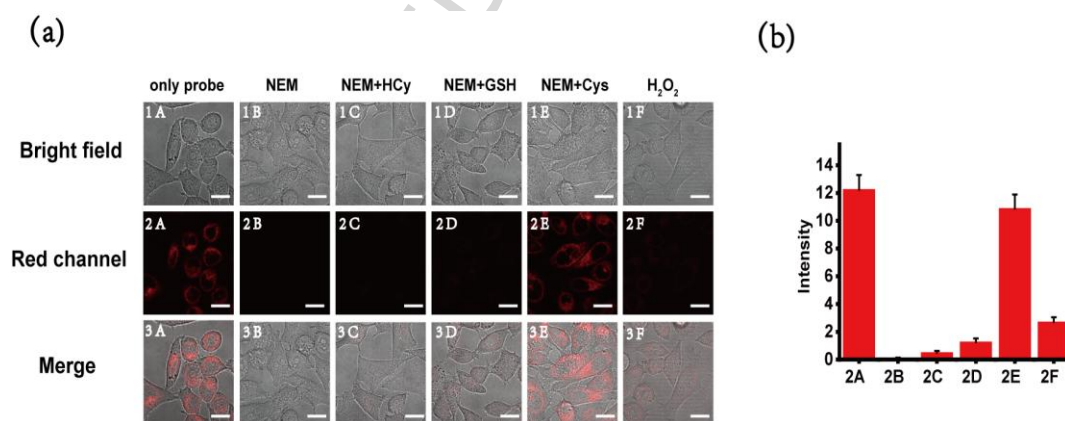


**Figure 6.** Confocal fluorescence images of Cys in living HeLa cells. (a) (2A): HeLa cells incubated with 10  $\mu\text{M}$  **CP** for 30 min. (2B): HeLa cells pretreated with 1.0 mM NEM for 30 min and then incubated with 10  $\mu\text{M}$  **CP** for 30 min. (2C, 2D, 2E) :HeLa cells pretreated with 1.0 mM NEM for 30 min and then incubated with 50  $\mu\text{M}$  Hcy, 1.0 mM GSH, and 50  $\mu\text{M}$  Cys for 1 h, respectively, and finally incubated with 10  $\mu\text{M}$

**CP** for 30 min. (2F): HeLa cells pretreated with 100  $\mu\text{M}$   $\text{H}_2\text{O}_2$  for 30 min and then incubated with 10  $\mu\text{M}$  **CP** for 30 min. Scale bar: 20  $\mu\text{m}$ . Channel 1A-1F and 3A-3F are the corresponding bright-field and merge image of 2A-2F, respectively. (b) The quantified mean intensity of channel 2A-2F obtained by image J software.

#### 4. Conclusion

In summary, a novel red-emitting fluorescent probe, namely, **CP**, was developed for the highly selective detection of Cys in living cells. This probe was designed based on the conjugated addition and intramolecular cyclization mechanism. By exploiting the difference in reaction kinetics, **CP** could distinguish Cys from Hcy and GSH directly. In addition, the rapid response (4 min), high sensitivity (147-fold fluorescence enhancement), and noteworthy Stokes shift (141 nm) contributed to the appreciable sensing properties of **CP** toward Cys. In view of the excellent sensing performance in solution and the low cytotoxicity, **CP** was successfully applied in the real-time monitoring of Cys level in living HeLa cells. Overall, this work provided a potential red-emitting fluorescent probe for the real-time and highly selective detection of Cys in biological systems.

#### ACKNOWLEDGMENT

This research was financially supported by the National Natural Science Foundation of China (Grant Number. 21878041, U1608222).

#### AUTHOR INFORMATION

##### Corresponding Author

\*E-mail: wangjingyun67@dlut.edu.cn. Tel: +86-41184706356

#### Notes

The authors declare no competing financial interest.

## Reference

- [1] E. Weerapana, C. Wang, G. M. Simon, F. Richter, S. Khare, M. B. D. Dillon, et al., Quantitative reactivity profiling predicts functional cysteines in proteomes, *Nature* 468(2010) 790.
- [2] C. E. Paulsen, K. S. Carroll, Cysteine-mediated redox signaling: chemistry, biology, and tools for discovery, *Chem. Rev.* 113(2013) 4633-4679.
- [3] Y. Yue, F. Huo, P. Ning, Y. Zhang, J. Chao, X. Meng, et al., Dual-Site Fluorescent Probe for Visualizing the Metabolism of Cys in Living Cells, *J. Am. Chem. Soc.* 139(2017) 3181-3185.
- [4] H. S. Jung, J. H. Han, T. Pradhan, S. Kim, S. W. Lee, J. L. Sessler, et al., A cysteine-selective fluorescent probe for the cellular detection of cysteine, *Biomaterials* 33(2012) 945-953.
- [5] M. W. Lieberman, A. L. Wiseman, Z. Z. Shi, B. Z. Carter, R. Barrios, C. N. Ou, et al., Growth retardation and cysteine deficiency in gamma-glutamyl transpeptidase-deficient mice, *Proc. Natl. Acad. Sci. USA* 93(1996) 7923-7926.
- [6] S. Shahrokhian, Lead phthalocyanine as a selective carrier for preparation of a cysteine-selective electrode, *Anal. Chem.* 73(2001) 5972-5978.
- [7] K. Reddie, K. Carroll, Expanding the functional diversity of proteins through cysteine oxidation, *Curr. Opin. Chem. Biol.* 12(2008) 746-754.
- [8] M. R. Housaindokht, J. Chamani, A. A. Saboury, A. A. Moosavi-Movahedi, M. Bahrololoom, Three Binding Sets Analysis of  $\alpha$ -Lactalbumin by Interaction of Tetradecyl Trimethyl Ammonium Bromide. *Bull. Korean Chem. Soc.* 22(2001) 145-148.
- [9] T. Shirin Hamed-Akbari, R. S. Mohammad, J. Chamani, Comparing the Interaction of Cyclophosphamide Monohydrate to Human Serum Albumin as Opposed to Holo-Transferrin by Spectroscopic and Molecular Modeling Methods: Evidence for Allocating the Binding Site. *Protein Peptide Lett.* 17(2010) 1524-1535.
- [10] B. Bakaeen, M. Kabiri, H. Iranfar, M. R. Saberi, J. Chamani, Binding Effect of Common Ions to Human Serum Albumin in the Presence of Norfloxacin: Investigation with Spectroscopic and Zeta Potential Approaches. *J. Solution Chem.* 41(2012) 1777-1801.
- [11] T. Sohrabi, M. Hosseinzadeh, S. Beigoli, M. R. Saberi, J. Chamani, Probing the binding of lomefloxacin to a calf thymus DNA-histone H1 complex by multi-spectroscopic and molecular modeling techniques. *J. Mol. Liq.* 256(2018) 127-138.
- [12] S. Rashidipour, S. Naeeminejad, J. Chamani, Study of the interaction between DNP and DIDS with human hemoglobin as binary and ternary systems: spectroscopic and molecular modeling investigation, *J. Biomol. Struct. Dyn.* 34(2016) 57-77.
- [13] Z. Sharif-Barfeh, S. Beigoli, S. Marouzi, A. S. Rad, A. Asoodeh, J. Chamani, Multi-spectroscopic and HPLC Studies of the Interaction Between Estradiol and Cyclophosphamide With Human Serum Albumin: Binary and Ternary Systems, *J. Solution Chem.* 46(2017) 488-504.

- [14] L. W. Zhang, M. Qian, J. Xia, L. L. Chen, H. Y. Cui, Y. Xia, L. Xu, J. Y. Wang, X. J. Peng, A NIR fluorescent sensor with large Stokes shift for the real-time visualization of endogenous hydrogen peroxide in living cells. *J. Photoch. Photobio. A* 370(2019) 12–17.
- [15] T. Peng, N. K. Wong, X. M. Chen, Y. K. Chan, D. H. Ho, Z. N. Sun, J. J. Hu, J. G. Shen, H. El-Nezami, D. Yang, Molecular imaging of peroxyxynitrite with HKGreen-4 in live cells and tissues. *J. Am. Chem. Soc.* 136(2014) 11728-11734.
- [16] H. D. Li, Q. C. Yao, J. L. Fan, N. Jiang, J. Y. Wang, J. Xia, X. J. Peng, A fluorescent probe for H<sub>2</sub>S in vivo with fast response and high sensitivity. *Chem. Commun.* 51( 2015) 16225-16228.
- [17] F. Ali, S. Sreedharan, A. H. Ashoka, H. K. Saeed, C. G. W. Smythe, J. A. Thomas, A. Das, A Super-Resolution Probe To Monitor HNO Levels in the Endoplasmic Reticulum of Cells. *Anal. Chem.* 89(2017) 12087-12093.
- [18] H. Zhang, J. L. Fan, J. Y. Wang, S. L. Zhang, B. R. Dou, X. J. Peng, An Off-On COX-2-Specific Fluorescent Probe: Targeting the Golgi Apparatus of Cancer Cells, *J. Am. Chem. Soc.* 135(2013) 11663-11669.
- [19] H. Zhu, J. L. Fan, J. Y. Wang, H. Y. Mu, X. J. Peng, An “enhanced PET”-based fluorescent probe with ultrasensitivity for imaging basal and elesclomol-induced HClO in cancer cells, *J. Am. Chem. Soc.* 136(2014) 12820-12823.
- [20] X. J. Liu, D. L. Yang, W. Q. Chen, L. Yang, F. P. Qi, X. Z. Song, A red-emitting fluorescent probe for specific detection of cysteine over homocysteine and glutathione with a large Stokes shift, *Sensor. Actuat. B-Chem.* 234(2016) 27-33.
- [21] C. Han, H. Yang, M. Chen, Q. Su, W. Feng, F. Li, Mitochondria-targeted near-infrared fluorescent off-on probe for selective detection of cysteine in living cells and in vivo, *ACS Appl. Mater. Inter.* 7(2015) 27968-27975.
- [22] T. Liu, F. J. Huo, J. F. Li, J. B. Chao, Y. B. Zhang, C. X. Yin, An off-on fluorescent probe for specifically detecting cysteine and its application in bioimaging, *Sensor. Actuat. B-Chem.* 237(2016) 127-132.
- [23] W. F. Niu, L. Guo, Y. H. Li, S. M. Shuang, C. Dong, M. S. Wong, Highly selective two-photon fluorescent probe for ratiometric sensing and imaging cysteine in mitochondria, *Anal. Chem.* 88(2016) 1908-1914.
- [24] S. M. Feng, Y. Fang, W. Y. Feng, Q. F. Xia, G. Q. Feng, A colorimetric and ratiometric fluorescent probe with enhanced near-infrared fluorescence for selective detection of cysteine and its application in living cells, *Dyes Pigments* 146(2017) 103-111.
- [25] D. Gong, Y. Tian, C. Yang, A. Iqbal, Z. Wang, W. Liu, et al., A fluorescence enhancement probe based on BODIPY for the discrimination of cysteine from homocysteine and glutathione, *Biosens. Bioelectron.* 85(2016) 178-183.
- [26] X. J. Wei, X. L. Yang, Y. Feng, P. Ning, H. Z. Yu, M. Z. Zhu, et al., A TICT based two-photon fluorescent probe for cysteine and homocysteine in living cells, *Sensor. Actuat. B-Chem.* 231(2016) 285-292.
- [27] P. Yue, X. Yang, P. Ning, X. Xi, H. Yu, Y. Feng, et al., A mitochondria-targeted ratiometric two-photon fluorescent probe for detecting intracellular cysteine and homocysteine, *Talanta* 178(2017) 24-30.

- [28] X. F. Hou, Z. S. Li, B. L. Li, C. H. Liu, Z. H. Xu, An "off-on" fluorescein-based colorimetric and fluorescent probe for the detection of glutathione and cysteine over homocysteine and its application for cell imaging, *Sensor. Actuat. B-Chem.* 260(2018) 295-302.
- [29] Y. Li, K. N. Wang, B. Liu, X. R. Lu, M. F. Li, L. N. Ji, et al., Mitochondria-targeted two-photon fluorescent probe for the detection of biothiols in living cells, *Sensor. Actuat. B-Chem.* 255(2018) 193-202.
- [30] K. Wang, T. Leng, Y. Liu, C. Wang, P. Shi, Y. Shen, et al., A novel near-infrared fluorescent probe with a large Stokes shift for the detection and imaging of biothiols, *Sensor. Actuat. B-Chem.* 248(2017) 338-345.
- [31] Y. Wang, L. Wang, E. Jiang, M. Zhu, Z. Wang, S. Fan, et al., A colorimetric and ratiometric dual-site fluorescent probe with 2,4-dinitrobenzenesulfonyl and aldehyde groups for imaging of aminothiols in living cells and zebrafish, *Dyes Pigments*, 156(2018) 338-347.
- [32] S. H. Xue, S. S. Ding, Q. S. Zhai, H. Y. Zhang, G. Q. Feng, A readily available colorimetric and near-infrared fluorescent turn-on probe for rapid and selective detection of cysteine in living cells, *Biosens. Bioelectron.* 68(2015) 316-321.
- [33] J. Guo, Z. Y. Kuai, Z. X. Zhang, Q. B. Yang, Y. M. Shan, Y. X. Li, A simple colorimetric and fluorescent probe with high selectivity towards cysteine over homocysteine and glutathione, *RSC Adv.* 7(2017) 18867-18873.
- [34] Y. L. Meng, Z. H. Xin, Y. J. Jia, Y. F. Kang, L. P. Ge, C. H. Zhang, et al., A near-infrared fluorescent probe for direct and selective detection of cysteine over homocysteine and glutathione, *Spectrochim. Acta A* 202(2018) 301-304.
- [35] H. M. Lv, D. H. Yuan, W. P. Liu, Y. Chen, C. T. Au, S. F. Yin, A highly selective ES IPT-based fluorescent probe for cysteine sensing and its bioimaging application in living cells, *Sensor. Actuat. B-Chem.* 233(2016) 173-179.
- [36] L. L. Xia, Y. Zhao, J. X. Huang, Y. Q. Gu, P. Wang, A fluorescent turn-on probe for highly selective detection of cysteine and its bioimaging applications in living cells and tissues, *Sensor. Actuat. B-Chem.* 270(2018) 312-317.
- [37] A. Y. Bochkov, I. O. Akchurin, O. A. Dyachenko, V. F. Traven, NIR-fluorescent coumarin-fused BODIPY dyes with large Stokes shifts, *Chem. Commun.* 49(2013) 11653-11655.
- [38] L. Yuan, W. Lin, K. Zheng, L. He, W. Huang, Far-red to near infrared analyte-responsive fluorescent probes based on organic fluorophore platforms for fluorescence imaging, *Chem. Soc. Rev.* 42(2013) 622-661.
- [39] Z. Guo, S. Park, J. Yoon, I. Shin, Recent progress in the development of near-infrared fluorescent probes for bioimaging applications, *Chem. Soc. Rev.* 43(2014) 16-29.
- [40] D. Su, J. Oh, S. C. Lee, J. M. Lim, S. Sahu, X. Yu, et al., Dark to light! A new strategy for large Stokes shift dyes: coupling of a dark donor with tunable high quantum yield acceptors, *Chem. Sci.* 5(2014) 4812-4818.
- [41] K. Gu, Y. Liu, Z. Guo, C. Lian, C. Yan, P. Shi, et al., In situ ratiometric quantitative tracing of intracellular leucine aminopeptidase activity via an activatable near-infrared fluorescent probe, *ACS Appl. Mater. Inter.* 40(2016) 26622-26629.

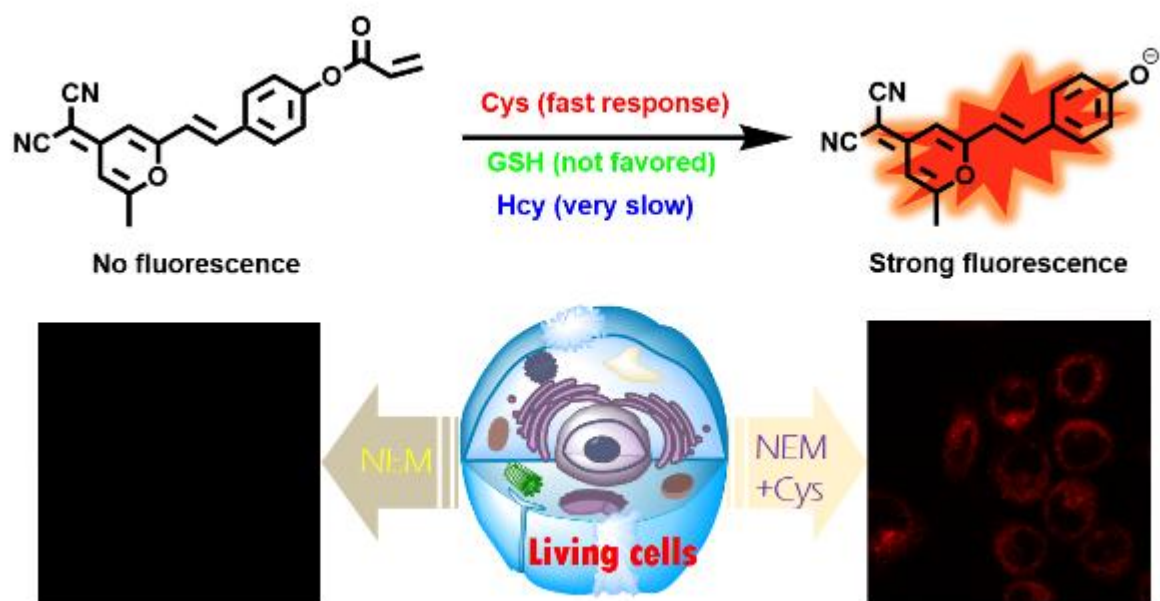
- [42] K. Gu, Y. Xu, H. Li, Z. Guo, S. Zhu, S. Zhu, et al., Real-time tracking and in vivo visualization of beta-galactosidase activity in colorectal tumor with a ratiometric near-infrared fluorescent probe, *J. Am. Chem. Soc.* 138(2016) 5334-5340.
- [43] J. X. Wang, C. Zhou, W. Liu, J. J. Zhang, X. Y. Zhu, X. Y. Liu, et al., A near-infrared fluorescent probe based on chloroacetate modified naphthofluorescein for selectively detecting cysteine/homocysteine and its application in living cells, *Photoch. Photobio.* 15(2016) 1393-1399.
- [44] Y. F. Kang, H. X. Qiao, Y. L. Meng, Z. H. Xin, L. P. Ge, J. N. Zheng, et al., A simple and sensitive fluorescent probe for specific detection of cysteine, *J. Chem. Sci.* 129(2017) 1219-1223.
- [45] S. J. Li, Y. J. Fu, C. Y. Li, Y. F. Li, L. H. Yi, O. Y. Juan, A near-infrared fluorescent probe based on BODIPY derivative with high quantum yield for selective detection of exogenous and endogenous cysteine in biological samples, *Anal. Chim. Acta* 994(2017) 73-81.
- [46] W. T. Dou, Y. Lv, C. Tan, G. R. Chen, X. P. He, Irreversible destruction of amyloid fibril plaques by conjugated polymer based fluorogenic nanogrenades, *J. Mater. Chem. B* 4(2016) 4502-4506.
- [47] X. Wang, W. Li, W. Li, C. Gu, H. Zheng, Y. Wang, et al., An RGB color-tunable turn-on electrofluorochromic device and its potential for information encryption, *Chem. Commun.* 53(2017) 11209-11212.
- [48] H. S. Seo, H. J. Kim, A Pyrone-based ratiometric probe for galactosidase with dramatic color and fluorescence changes, *B. Korean Chem. Soc.* 38(2017) 1134-1137.
- [49] C. Yan, Z. Guo, Y. Shen, Y. Chen, H. Tian, W. H. Zhu, Molecularly precise self-assembly of theranostic nanoprobes within a single-molecular framework for: in vivo tracking of tumor-specific chemotherapy, *Chem. Sci.* 9(2018) 4959-4969.
- [50] L. Chen, M. Qian, L. Zhang, J. Xia, Y. Bao, J. Wang, et al., Co-delivery of doxorubicin and shRNA of Beclin1 by folate receptor targeted pullulan-based multifunctional nanomicelles for combinational cancer therapy, *RSC Adv.* 8(2018) 17710-17722.
- [51] J. Xia, L. Zhang, M. Qian, Y. Bao, J. Wang, Y. Li, Specific light-up pullulan-based nanoparticles with reduction-triggered emission and activatable photoactivity for the imaging and photodynamic killing of cancer cells, *J. Colloid Interf. Sci.* 498(2017) 170-181. (52) J. Zhang, F. Pan, Y. Jin, N. Wang, J. He, W. Zhang, et al., A BODIPY-based dual-responsive turn-on fluorescent probe for NO and nitrite, *Dyes Pigments*, 155(2018) 276-283.
- [53] R. R. Nawimanager, B. Prasai, S. U. Hettiarachchi, R. L. McCarley, Cascade reaction-based, near-infrared multiphoton fluorescent probe for the selective detection of cysteine, *Anal. Chem.* 89(2017) 6886-6892.
- [54] Y. W. Yu, J. J. Yang, X. H. Xu, Y. L. Jiang, B. X. Wang, A novel fluorescent probe for highly sensitive and selective detection of cysteine and its application in cell imaging, *Sensor. Actuat. B-Chem.* 251(2017) 902-908.
- [55] S. J. Li, Y. J. Fu, C. Y. Li, Y. F. Li, L. H. Yi, J. Ou-Yang, A near-infrared fluorescent probe based on BODIPY derivative with high quantum yield for selective detection of

---

exogenous and endogenous cysteine in biological samples. *Anal. Chim. Acta* 994(2017) 73-81.

ACCEPTED MANUSCRIPT

## Graphic abstract



---

**Highlights**

- > A red-emitting fluorescent probe **CP** with large Stokes shift was developed.
- > **CP** can discriminate cysteine from glutathione and homocysteine in the solution and living cells.
- > **CP** shows rapid response and high sensitivity toward cysteine.
- > The limit of detection was as low as 41.696 nM.
- > **CP** can monitor the exogenous and endogenous cysteine in living cells.